

# Metal Flux and Dynamic Speciation at (Bio)Interfaces. Part IV: MHEDYN, a General Code for Metal Flux Computation; Application to Particulate Complexants and Their Mixtures with the Other Natural Ligands

DAVIDE ALEMANI, JACQUES BUFFLE,\*  
AND ZESHI ZHANG

CABE, Department of Inorganic, Analytical and Applied  
Chemistry, Sciences II, 30 quai E. Ansermet, 1211 Geneva 4,  
Switzerland

JOSEP GALCERAN

Department de Química, Universitat de Lleida, av. Rovira  
Roure 191, 25198 Lleida, Spain

BASTIEN CHOPARD

Department of Computer Science, University of Geneva,  
Switzerland

Received June 4, 2007. Revised manuscript received  
November 30, 2007. Accepted December 6, 2007.

Metal flux at consuming interfaces (e.g., sensors or microorganisms) is simulated in environmental multiligand systems using a new numerical code, MHEDYN (Multispecies Heterogeneous DYNamics), based on the lattice Boltzmann method. The attention is focused on the computation of the maximum flux (i.e., the flux controlled by diffusion—reaction in solution) of Cu(II). Part III described flux computation in the presence of simple ligands and fulvic/humic substances. This paper (Part IV) discusses the case of metal complexes formed with aggregates including a broad range of sizes and diffusion coefficients and their mixture with simple and fulvic ligands under typical natural water conditions. This paper describes the dynamic contribution of the various size classes of aggregate Cu(II) complexes for the first time. In two typical waters containing mixtures of ligands, the contribution of aggregates is found to be small, whereas that of fulvics may play a major role, even under pH conditions where the lability of their Cu(II) complexes is low. These results point out the great usefulness of MHEDYN for dynamic speciation in very complex mixtures. In all cases, MHEDYN enables us to compute the concentration profile of each complex and its time evolution, as well as the steady-state flux and the corresponding contribution of each complex to the flux. Thus, MHEDYN should be very useful for comparing theoretical predictions with experimental measurements of metal bioavailability or of dynamic sensor response in a complete aquatic medium.

## 1. Introduction

As explained in ref 1, Parts III and IV of this series have two major goals: (i) to show how the new code MHEDYN (Multispecies Heterogeneous DYNamics), developed on the principles explained in refs 1–4, is applicable for transient and steady-state metal flux computations at consuming interfaces such as dynamic sensors (5, 6) or organisms (7) in environmentally realistic mixtures of ligands, and (ii) to study the relative role of each individual natural complex on the steady-state flux.

As discussed in part III, natural complexants can be classified into three categories (8, 9): (a) the so-called simple organic and inorganic ligands, such as  $\text{OH}^-$ ,  $\text{CO}_3^{2-}$ , aminoacids, or oxalate, which bind to metals via classical electrostatic and covalent forces; (b) the organic biopolymers, in particular the humic/fulvic compounds, which are chemically heterogeneous, with polyelectrolytic properties and can be treated as monodispersed macromolecules, and (c) the colloidal particles and aggregates, which form coordination surface complexes. Their important reactive sites (e.g.,  $\equiv\text{FeOOH}$  sites on iron oxide) form complexes with intermediate to strong stability and intermediate to slow chemical kinetics. In addition, natural particles/aggregates are broadly polydispersed, with sizes in the range 1–1000 nm. Thus, their contribution to metal bioavailability is not straightforwardly predicted.

Part III (1) has discussed the computation of metal flux in the presence of simple ligands and fulvic substances separately. This paper shows, first, how MHEDYN can be applied to compute metal fluxes in the presence of particulate/aggregate complexants and also to estimate the relative contribution of each size fraction of complexes to the overall flux. In a second part of the paper (Section 3), MHEDYN is applied to the computation of metal flux in typical natural freshwaters, containing mixtures of simple ligands, fulvics, and aggregates, to understand the role of each type of complex on metal availability. The effect of stirring (which influences the diffusion layer thickness) is also briefly discussed.

In all cases, as in Part III (1), the so-called maximum flux is computed. It only depends on diffusion and chemical reactions in solution and not on the metal transfer at the consuming interface. As discussed in ref 1, the maximum flux is a key piece of information, complementary to the minimum flux provided by FIAM and BLM models, and is equally required to characterize an aquatic system with respect to bioavailability and ecotoxicology of metals.

## 2. Metal Flux in Presence of Suspended Particles/Aggregates

**2.1. Simulation Conditions.** Environmental “particles” are often aggregates of inorganic colloids and biopolymers whose chemical homogeneity is highly variable. As discussed in detail elsewhere (9), they are considered below as fractal aggregates with fractal dimension  $D_f$ . In addition, they are considered as chemically homogeneous (i.e., containing only one type of complexing site), in order to specifically study the role of aggregate size distribution on the metal flux. The goals of the following simulations are to evaluate (i) the degree of lability ( $l^\xi$ ) (1, 10) of the complexes in the various size classes ( $j$ ) having different radii ( $r_j$ ) and diffusion coefficients ( $D_j$ ) at steady state, and (ii) the size classes of complexes that play the most important role on the total steady-state flux ( $J_t$ ), based on computations of the individual fluxes ( $J_j$ ) of the

\* Corresponding author telephone: ++41 22 3796053; fax ++41 22 3796069; e-mail: Jacques.Buffle@cabe.unige.ch.

**TABLE 1. Parameters Used and Computed Total Fluxes for Cu(II) Flux Simulations with Particles/Aggregates<sup>a</sup>**

input parameters	case E	case F
[Cu] <sub>t</sub> (M)	10 <sup>-7</sup>	10 <sup>-7</sup>
[L] <sub>t</sub> (M)	1.66 × 10 <sup>-5</sup>	1.66 × 10 <sup>-7</sup>
{FeOOH} (mg/dm <sup>3</sup> )	3	0.03
[Cu]/[L]/[Cu] <sub>t</sub>	100%	99.7%
pH	8	8
r <sub>min</sub> (nm)	3.4	3.4
r <sub>max</sub> (nm)	894.3	894.3
Log K'	9.68	9.68
β	3	3
D <sub>f</sub>	2	2
computed fluxes		
J <sub>t</sub> (mol m <sup>-2</sup> s <sup>-1</sup> )	2.59 × 10 <sup>-13</sup>	1.91 × 10 <sup>-11</sup>
J <sub>lab</sub> (mol m <sup>-2</sup> s <sup>-1</sup> )	6.12 × 10 <sup>-11</sup>	7.20 × 10 <sup>-11</sup>

<sup>a</sup> T = 25 °C, ionic strength = 0.01M, δ = 21 μm. K' is the apparent stability constant at pH = 8 and under the conditions used; it is expressed as K' = [ML]/[M][L]. Ψ = 0 mV in both cases. For other conditions, see text.

complexes. For that purpose, distributions of  $j/J_t$  and  $i\xi$  as a function of  $\log^j D$  or  $\log^j r$  are presented (Figure 1, panels a and b).

The physicochemical model of aggregates and their metal complexes described in ref 9 will be used below. In this section, the aggregates are supposed to be composed of solid "basic" subparticles, which bear surface complexing sites forming a single type of 1/1 complex with Cu(II). A typical value of the stability constant for Cu(II) complexes with natural aggregates has been used (9), which is close to that of the complex formed with ≡FeOOH sites. For that reason, the aggregate mass concentration is expressed as the mass of FeOOH per liter, {FeOOH}, and the site concentration is computed from the density of am-FeOOH, as discussed in eqs 15 and 16 in ref 9. The number of sites in each size class is assumed to be proportional to the surface area of that class (see below).

As usually found in natural waters (11), the size distribution of the aggregates is supposed to be continuous and to follow a Pareto law (eq 1),

$$dc_p/dr \propto r^{-\beta} \quad (1)$$

where  $c_p$  is the number concentration of aggregates, and  $r$  is their radius.  $\beta$  is a constant, often close to 3 for a given system (9). Such a function implies that small sized aggregates are much more numerous than large ones. They diffuse faster, but they transport fewer metal complexes per aggregate. Because the total complexing site concentration ( $IL_t$ ) is much larger than  $ICu_t$ , the fraction of bound Cu(II) in each size class is proportional to the fraction ( $\Delta A/A_t$ ) of the surface area inside each size class of aggregate. It can be computed from eq 2 below, when  $\beta = 3$  and  $D_f = 2$  (which is realistic in many aquatic systems (9)).

$$\frac{\Delta A}{A_t} = \frac{\Delta \log r}{\log(r_{\max}/r_{\min})} = \frac{\Delta \log D}{\log(D_{\max}/D_{\min})} \quad (2)$$

In eq 2,  $r_{\min}$  and  $r_{\max}$  are the minimum and maximum radii of the aggregates, and  $D_{\max}$  and  $D_{\min}$  are the corresponding maximum and minimum values of diffusion coefficients.  $\Delta \log r$  or  $\Delta \log D$  is the absolute value of the arbitrarily chosen width of the size classes ( $\Delta \log D = 0.097$  has been used here). Eq 2 implies that, under this condition, each class has the same amount of Cu(II). Note that, below,  $J_t$  is used to denote the complexing sites present in the size class  $j$ .

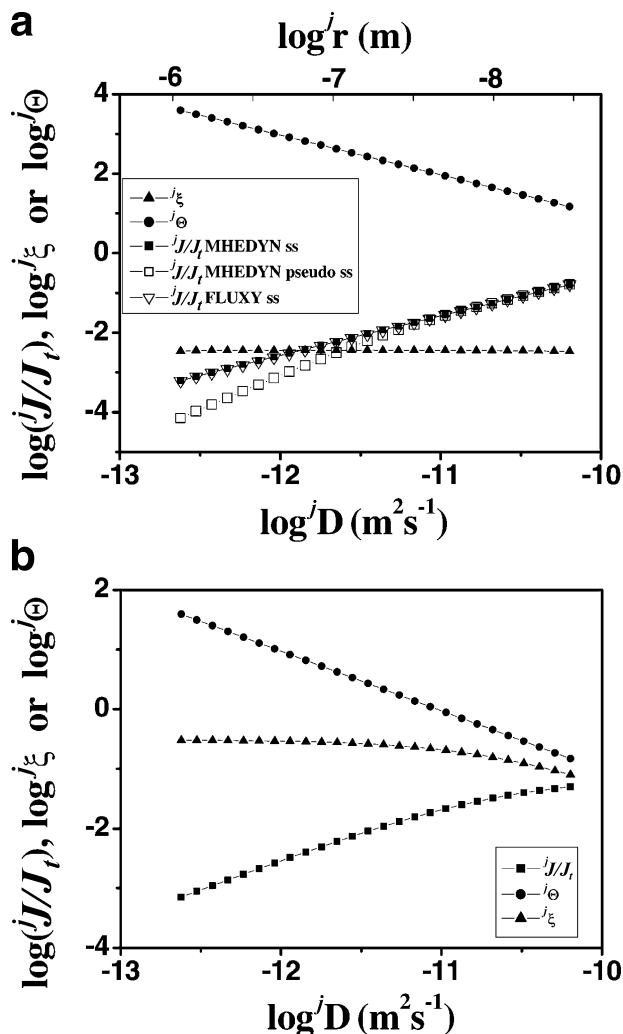


**FIGURE 1. (a) Steady-state lability degree and individual flux distributions as a function of the aggregate's size class for {FeOOH} = 3 mg/dm<sup>3</sup> (case E). Full triangle,  $i\xi$ ; Full circle,  $i\theta$ ; Open triangle,  $j/J_t$  computed with FLUXY (steady-state = ss); Full square,  $j/J_t$  computed with MHEDYN at ss; Open squares,  $j/J_t$  computed with MHEDYN at pseudo ss (pseudoss). The last two curves are obtained by stopping computation after 30 min (ss) and 3 min (pseudoss). In both cases,  $J_t$  has reached a value independent of time. However, after 3min, a true steady-state is reached only for the smaller size particles (which contribute predominantly to  $J_t$ ). The results obtained with MHEDYN and FLUXY at true steady-state are indistinguishable. Simulation parameters in Table 1 and Supporting Information Table S1. (see ref 1 for details on FLUXY). (b) Lability degree and individual flux distributions as a function of the aggregate's size class for {FeOOH} = 30 μg/dm<sup>3</sup> (case F). Full triangle,  $i\xi$ ; Full circle,  $i\theta$ ; Full square,  $j/J_t$  computed with MHEDYN. FLUXY cannot be used in case F because the site concentration is not in excess with respect to Cu(II). Parameters as in Table 1 and Supporting Information Table S2.**

As discussed in ref 9, the overall formation rate of a Cu(II) complex with an aggregate site depends on three processes: the diffusion of free Cu outside and inside the aggregate, the formation of an outer-sphere complex with a complexing site, and the elimination of a water molecule from the inner hydration shell of the metal ion. It can be shown (9) that the combination of these processes lead, at steady-state, to an overall formation rate constant ( $k_a$ ) smaller than or equal to that occurring with small size simple ligands. It is given by eq 3 (9),

$$j_{k_a} = \frac{k_a^{MS}}{1 + \frac{k_a^{MS}[L]_t(\Delta A/A_t)}{4\pi r D_M j_c p}} = \frac{k_a^{MS}}{1 + j\Theta} \quad (3)$$

and the corresponding dissociation rate constant is obtained via  $j_{k_d} = j_{k_a}/jK$ . In eq 3,  $[L]_t$  is the total coarse-grained concentration of complexing sites in the bulk solution, and  $k_a^{MS}$  is the “intrinsic” formation rate constant of the metal complex with an aggregate site. It is obtained by combining the formation and dissociation rates of the outer-sphere complex formed between M and the complexing site, and the dehydration rate of free M (8, 9). When an electrical field develops at the surface of the adsorbing solid, the corresponding potential at the complexing site is also considered in the computation of  $k_a^{MS}$ . In eq 3,  $j\Theta$  is a “correction” term taking into account the diffusion of M between the solution and the aggregate sites. Note that, even though  $k_a^{MS}$  is independent of the size class  $j$ , the effective rate constant  $j_{k_a}$  depends on this size through both  $j_r$  (or  $jD$ ) and the number concentration of aggregates in the size class  $j$ . (The symbol  $j_{k_a}$ , instead of  $j_{k_a}^{eff}$  used in ref 9, is employed here for consistency in the mathematical formulation of the problem involving mixtures of ligands; Section A in the Supporting Information of ref 1.)

Two cases (E and F) corresponding to stronger and weaker Cu(II) complexation are discussed below, with the conditions given in Table 1. All other parameters are listed in Supporting Information Tables S1 and S2.  $D_{min}$  and  $D_{max}$  are  $2.39 \times 10^{-13}$  and  $6.38 \times 10^{-11} \text{ m}^2 \text{ s}^{-1}$ , respectively, corresponding to  $r_{max} = 894.3 \text{ nm}$  and  $r_{min} = 3.4 \text{ nm}$ , respectively. This size range corresponds to that of colloidal ligands that are part of the “dissolved” ligands, because their sedimentation is very slow. For sizes smaller than a few nanometers, the number of complexing sites per particle/aggregate is too small for eq 3 to be applicable. The  $\Delta \log D$  value was 0.097, corresponding to 26 size classes in the whole range covered. Because  $[L]_t$  is lower in case F than in case E, it is expected that the degree of lability of the complexes will be larger.

**2.2. Simulation Results.** The study of the time evolution of the total flux ( $J_t$ ) (data not shown) indicates that the time needed to reach constant  $J_t$  values is about 30 s for  $\{\text{FeOOH}\} = 3 \text{ mg/L}$  and is 5 min for  $\{\text{FeOOH}\} = 30 \text{ } \mu\text{g/L}$ . However, a practically constant value of  $J_t$  is not always sufficient to ensure that a true steady-state is reached. A better test is performed by looking at the change of the curve  $\log(j/J_t)$  vs  $\log jD$  as a function of time, where  $jJ$  is the flux of the complexes in the class  $j$  (see Figure 1a and its legend for details). Steady-state is reached when  $jJ/J_t$  values are constant for all size classes, in particular the largest ones (Figure 1, panels a and b). Comparison of results of MHEDYN and FLUXY in Figure 1a is particularly interesting here. As discussed in ref 1, FLUXY (12) is another code for flux computation based on more limiting assumptions than MHEDYN but which specifically computes the steady-state flux. In cases E and F, it was observed that, for the largest aggregates ( $j_r$  close to 1000 nm), steady-state fluxes were obtained only after about 20 min. These times are significantly larger than those obtained with quickly diffusing molecules such as inorganic complexants, or even fulvic compounds. Nevertheless, they are still rather short when compared to many environmental processes.

Figure 1, panels a and b, shows the distributions of  $j\xi$  and  $jJ/J_t$  for all size classes. The degree of lability is significantly lower at a larger (Figure 1a) than at a low (Figure 1b) values of  $[L]_t$ . This is expected for any simple ligand (7, 13, 14) for which  $k_a$  is independent of  $[L]_t$ . But the effect is even more pronounced for complexes formed with aggregates, because  $[L]_t$  is included in the term  $j\Theta$  of eq 3, in such a way that  $j_{k_a}$

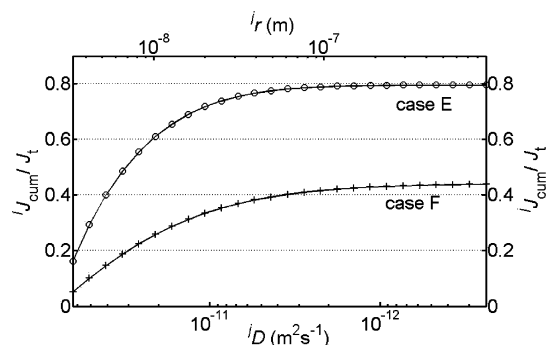


**FIGURE 2.** Cumulative fluxes of Cu complexes with aggregates as a function of their size class. Curve E corresponds to case E ( $\{\text{FeOOH}\} = 3 \text{ mg/dm}^3$ ), and curve F corresponds to case F ( $\{\text{FeOOH}\} = 30 \text{ } \mu\text{g/dm}^3$ ). Other parameters are as in Figure 1, Table 1, and Supporting Information Tables S1 and S2. For case E, the results of MHEDYN and FLUXY are superimposed.

decreases when  $[L]_t$  increases. Note that, even at low  $[L]_t$  (Figure 1b), the complexes are never fully labile ( $j\xi \leq 0.2$ ).

Comparison of panels a and b in Figure 1 shows that, for low  $[L]_t$ ,  $j\xi$  is constant in the low to intermediate  $jD$  range, and it decreases when  $jD$  increases in the large  $jD$  range; on the other hand, at large  $[L]_t$  it is constant for any aggregate size. These observations can be understood as a competition between two effects. On one hand, the lability of any complex increases with its size, because the ratio of the rates of chemical formation/dissociation reaction over diffusion becomes larger and larger (14). But with aggregate complexants,  $j_{k_a}$  simultaneously varies with  $j_r$  via the term  $j\Theta$ . For fractal aggregates, it has been shown (9) that  $j\Theta$  is proportional to  $r^{D_f-1}$ , that is, to  $r$  in the present case ( $D_f = 2$  is used here). This change compensates the above expected increase of lability degree. In summary, when  $j\Theta \ll 1$ ,  $j_{k_a}$  is independent of  $j$ , and the lability increases when the diffusion coefficient of the complex decreases (Figure 1b in the small size range). On the opposite side, when  $j\Theta \gg 1$ , then the increase of lability is compensated by the term  $j\Theta$ .

Panels a and b of Figure 1 show that, under the two presented conditions, the contribution ( $jJ$ ) of a given M/L complex to the overall flux ( $J_t$ ) decreases when  $j_r$  increases. Figure 2 shows the cumulative fluxes,

$$J_{cum} = \sum_{i=1}^j jJ$$

as a function of  $j_r$ , where the class indicated by  $i = 1$  corresponds to the smallest size class. It shows that only the complexes formed with the smallest size classes of aggregates (typically <10 to 20 nm) contribute significantly to the total flux. This is of major importance for understanding the role of the various environmental complexants in biouptake fluxes, because it suggests that most of the metal ions bound to colloids, that is, usually a major fraction of the total “dissolved” metal, are not bioavailable. It is also interesting to note that the sum of the individual fluxes of all complexes is significantly smaller than the total flux ( $J_t$ ) in both tested cases. This is due to the comparatively large diffusion coefficient of  $\text{Cu}^{2+}$  and the fact that it can be 100% consumed at the interface. As a consequence, free  $\text{Cu}^{2+}$  provides a significant contribution to  $J_t$ , even though its concentration ( $1.3 \times 10^{-12} \text{ M}$  in case E and  $3.1 \times 10^{-10} \text{ M}$  in case F) is very low compared to  $[\text{Cu}]_t$  ( $10^{-7} \text{ M}$  in both cases). The minor role of aggregate complexes on the total flux is also pointed out by the comparison of  $J_t$  and  $J_{lab}$ , that is, the steady-state flux that would be obtained if the complexes were fully labile while keeping their own mobility (i.e., unchanged diffusion



**TABLE 2. Summary of the main parameters used for simulation in water No. 1 and water No. 2. Parameters for hydroxo and carbonate complexes: see Table 1 of ref 1.  $\{P\}_t$  = total mass concentration of aggregates;  $\{FeOOH\}$  = mass concentration of the complexing component, FeOOH, of the aggregates. Surface potential at aggregate complexing sites = 0 mV. Potential difference between fulvic molecules and solution = -114 mV (1, 8)**

	water No. 1	water No. 2
$[Cu]_t$ (M)	$10^{-8}$	$3.5 \times 10^{-7}$
$[CO_3]_t$ (M)	$2 \times 10^{-3}$	$2 \times 10^{-3}$
$\{FS\}$ (mg C/dm <sup>3</sup> )	2	2
$\{FeOOH\}$ (mg/dm <sup>3</sup> )	0.03	0.3
$\{P\}_t$ (mg/dm <sup>3</sup> )	3	3
$\delta$ ( $\mu$ m)	20	20
$FSk_a$ (m <sup>3</sup> mol <sup>-1</sup> s <sup>-1</sup> )	$3.31 \times 10^7$	$3.29 \times 10^7$
$D_{FS}$ (m <sup>2</sup> s <sup>-1</sup> )	$2.80 \times 10^{-10}$	$2.80 \times 10^{-10}$
$\Gamma$	0.52	0.52
$\log K_0^*$	8.04	8.04
$\log K^*$	12.5	9.5
pH	8	8
$r_{min}$ (nm)	3.4	3.4
$r_{max}$ (nm)	894.3	894.3
$\log K'$ (aggregates)	9.68	9.68
$\beta$	3	3
$D_t$	2	2

coefficients). Table 1 shows that, in both cases E and F,  $J_i \ll J_{lab}$ . Thus, in mixtures where simple labile complexes are also present, it may be expected that the flux contribution of complexes with aggregates will be quite low (see Section 3), at least for aggregate complexes with  $r > 10$ –20 nm.

### 3. Metal Fluxes in Mixtures of Environmental Complexants

In this section the code MHEDYN has been used to compute the relative contributions to the total copper flux of each copper complex in environmental mixtures of hydroxide, carbonate, fulvic, and aggregate complexants. Fluxes have been computed in two "typical" natural waters with realistic compositions given in Tables 2 and 3 (A complete and detailed summary of the results of these simulations is given in ref 4). Note that, overall, 60 metal species with  $D$  values ranging from  $2 \times 10^{-13}$  to  $9 \times 10^{-10}$  m<sup>2</sup> s<sup>-1</sup> and with  $k_a$  values ranging from  $7 \times 10^2$  to  $2.5 \times 10^8$  m<sup>3</sup> mol<sup>-1</sup> s<sup>-1</sup> were treated by MHEDYN in each case.

In this section, fractal aggregates are assumed to be formed by an assembly of solid subparticles, with radius  $b = 3$  nm on which patches of an amorphous metal hydroxide layer of thickness  $h = 1$  nm are adsorbed as described in ref 9. The subparticles are supposed to be noncomplexing under the conditions used, and the metal hydroxide layer can form 1/1

complexes with stability constants typical for aquatic particles and close to those with FeOOH (9). For that reason, the mass concentration of the complexing solid is expressed as  $\{FeOOH\}$  in Table 2, and the corresponding molar site concentration is computed as explained in ref 9. The total mass concentration of aggregates is expressed as  $\{P\}_t$  in Table 2. The main difference with the aggregates discussed in Section 2 (composed of FeOOH only) is that, in the present case, the complexing surface area can be varied independently of the total mass of the aggregates.

In the two tested cases (water No. 1 and No. 2, Tables 2 and 3), the roles of fulvics and aggregates are expected to change, because (i) the copper-to-fulvic ratio increases from water No. 1 to 2, that is, the complexation strength of Cu(II) by fulvics significantly decreases and (ii) the overall concentration (and thus the complexing strength) of the aggregate complexing sites increases in the same order.

Most computations with waters No. 1 and 2 were performed with  $\delta = 20$   $\mu$ m. These results are discussed below. For comparison purposes, fluxes in water No. 2 were also computed with  $\delta = 50$   $\mu$ m and are discussed at the end of this section. The concentration profiles obtained for water No. 1 and No. 2, for each species, were similar to those obtained in Sections 3–4 of Part III (1) and in Section 2 of the present article and are not shown here. The time evolutions of the total fluxes were similar to those obtained with aggregates alone, confirming that reaction–diffusion with aggregates is also the slowest step in mixtures of aggregate and soluble ligands and that the overall time to reach a constant total flux should be at least of the order of minutes in environmental systems containing small size colloids. As already mentioned, the reaching of a steady-state flux in the presence of complexes with large size aggregates may take about 30 min, but their contribution to the flux is negligible.

Under similar conditions, the distributions of the lability degree ( $i\xi$ ) and of the individual steady-state flux ( $iJ$ ) of the fulvic complexes as a function of  $iK$  were similar in the mixture of ligands and in presence of fulvic compounds alone (1). The same observation was made for the distributions of  $i\xi$  and  $iJ$  with respect to  $iJ$  (or  $iD$ ) for complexes with aggregates. Thus, these results are not reported here. On the other hand, Figure 3 shows the cumulative fluxes,  $J_{cum} = \int iJ$  of the complexes with aggregates, in the two tested waters.

Comparison of Figures 2 and 3 is interesting; case F (Figure 2), water No. 1 (Figure 3), water No. 2 (Figure 3), and case E (Figure 2) correspond to increasing complexing strengths of aggregates for Cu(II). It can be seen that the aggregates that contribute the most to the total flux are always those with  $iJ \leq 10$ –20 nm, irrespective of complexation strength. Thus, even though more data are desirable, these results strongly suggest that the contribution of metal–aggregate complexes with sizes larger than 10–20 nm can be neglected in flux computations.

**TABLE 3. Steady-state fluxes and bulk concentrations, normalized with respect to  $[Cu]_t$ , of the species present in water n°1 and n°2. Parameters: see Table 2. Cu-Fulvics = sum of all fulvic complexes, Cu-aggregates = sum of all aggregate complexes, X = species (or sum of species) X**

species X	water No. 1, $\delta = 20$ $\mu$ m			water No. 2, $\delta = 20$ $\mu$ m			water No. 2, $\delta = 50$ $\mu$ m	
	$[X]/[Cu]_t$ (%)	$J_X$ (mol m <sup>-2</sup> s <sup>-1</sup> )	$J_X/J_t$ (%)	$[X]/[Cu]_t$ (%)	$J_X$ (mol m <sup>-2</sup> s <sup>-1</sup> )	$J_X/J_t$ (%)	$J_X$ (mol m <sup>-2</sup> s <sup>-1</sup> )	$J_X/J_t$ (%)
Cu <sup>2+</sup>	0.003	$1.04 \times 10^{-14}$	0.53	0.097	$1.21 \times 10^{-12}$	0.45	$4.03 \times 10^{-13}$	0.22
CuOH + Cu(OH) <sub>2</sub>	0.065	$6.03 \times 10^{-14}$	3.05	0.164	$8.19 \times 10^{-12}$	3.02	$4.08 \times 10^{-12}$	2.23
CuCO <sub>3</sub> + Cu(CO <sub>3</sub> ) <sub>2</sub>	0.128	$1.83 \times 10^{-13}$	9.28	0.305	$2.09 \times 10^{-11}$	7.68	$8.82 \times 10^{-12}$	4.82
Cu-Fulvics	97.50	$1.70 \times 10^{-12}$	86.9	33.14	$2.38 \times 10^{-10}$	87.5	$1.61 \times 10^{-10}$	88.0
Cu-Aggregates	2.317	$2.54 \times 10^{-15}$	0.19	66.49	$1.59 \times 10^{-12}$	0.58	$7.87 \times 10^{-12}$	4.3
$J_t$ (mol m <sup>-2</sup> s <sup>-1</sup> )		$1.97 \times 10^{-12}$	100		$2.72 \times 10^{-10}$	100	$1.83 \times 10^{-10}$	100
$J_t/J_{lab}$ (%)		1.44			14.9		30.0	

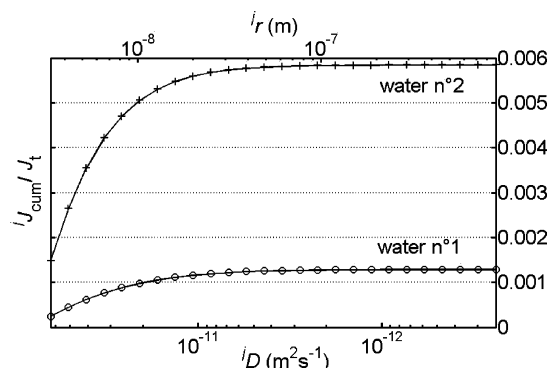


**FIGURE 3.** Cumulative fluxes of complexes, with aggregates, as a function of the radii and the diffusion coefficients of the aggregate class, for water No. 1 ( $\{\text{FeOOH}\} = 30 \mu\text{g}/\text{dm}^3$ ) and No. 2 ( $\{\text{FeOOH}\} = 300 \mu\text{g}/\text{dm}^3$ ). Parameters of water No. 1:  $[\text{Cu}]_i = 10^{-8} \text{ M}$ ,  $\{\text{FS}\} = 2 \text{ mg C}/\text{dm}^3$ ,  $\log K^* = 12.5$ ,  $[\text{CO}_3]_i = 2 \text{ mM}$  water No. 2:  $[\text{Cu}]_i = 3.5 \times 10^{-7} \text{ M}$ ,  $\{\text{FS}\} = 2 \text{ mg C}/\text{dm}^3$ ,  $\log K^* = 9.5 \text{ M}^{-1}$ ,  $[\text{CO}_3]_i = 2 \text{ mM}$ . For other parameters, see Tables 2 and 3.

Table 3 provides the steady-state fluxes due to free  $\text{Cu}^{2+}$ , carbonate complexes ( $\text{CuCO}_3^0 + \text{Cu}(\text{CO}_3)_2^{2-}$ ), hydroxo-complexes ( $\text{CuOH}^+ + \text{Cu}(\text{OH})_2^0$ ), fulvic complexes and aggregate complexes and their contribution (in %) to the total flux ( $J_t$ ) for water No. 1 and No. 2. It also provides, for comparison, the proportion of the various types of complexes in the mixture and the ratio of  $J_i/J_{\text{lab}}$ . It shows that, for both waters, the overall flux is largely dominated by the Cu–fulvic complexes. Among inorganic soluble complexes, the carbonate complexes  $\text{CuCO}_3$  and  $\text{Cu}(\text{CO}_3)_2$  are the most important under the conditions used, but their contribution to the total flux remains marginal (<10%). It must be emphasized, however, that this latter proportion is considerably larger than their proportion in  $[\text{Cu}]_i$  (<1%), due to their diffusion coefficient and lability that are much larger than those of fulvic or aggregate complexes.

The contribution of aggregate complexes to the total flux is negligible for both waters. This is worth emphasizing, because the complexing strengths of their sites have been increased by 10 times ( $\{\text{FeOOH}\}$  is 10 times larger) and the total Cu concentration has been increased by 35 times, in water No. 2 compared to water No. 1. As a consequence, the total concentration of aggregate complexes, with respect to the total concentration of Cu, is 2.3% for water No. 1 and is 66.5% for water No. 2. At the same time, the complexation strength of the fulvics decreases by a factor of  $35^{1/\Gamma} = 923$  (eq 4 in ref 1) due to the increase of the metal/fulvic ratio by a factor of 35. Consequently, the bulk concentration of fulvic complexes decreases from 97.5 to 33%. Even though all these conditions should favor the contribution of aggregates to the overall flux compared to fulvics, these latter still dominate. This is largely due to their respective degree of lability: that of aggregates decreases in water No. 2 in comparison with water No. 1 due to the increase of complexing site concentration. Simultaneously, the degree of lability of fulvic complexes drastically increases in water No. 2, due to the increase of the metal-to-ligand ratio.

For comparison, the individual flux contribution of each species to the total flux in water No. 2, has also been computed for a diffusion layer thickness of  $50 \mu\text{m}$ , instead of  $20 \mu\text{m}$ . Note that, as expected, all complexes become more labile ( $J_i/J_{\text{lab}} = 30\%$  instead of  $15\%$ ). Interestingly, however, the relative contribution of fulvic complexes is almost unchanged (88%), and changes of the other relative contributions are small. That of the aggregate complexes increases from 0.6 to 4.3% but remains marginal. Thus, the present results suggest that, as the diffusion layer becomes thicker, the flux contribution of the aggregate complexes increases, mostly

at the expense of those of simple complexes, but these changes are small in the range  $\delta = 20\text{--}50 \mu\text{m}$ . The whole of these results suggests that the contribution of Cu-complexes with particles/aggregates is usually small, even though it depends on the diffusion layer thickness, whereas the contribution of Cu–fulvic complexes is very significant or even predominant depending on conditions. For fluxes at microorganisms, spherical diffusion must be considered, but similar conclusions can be expected.

## Definitions of Symbols

$A$ , surface area of particle/aggregates ( $\text{m}^2$ );  $c_p$ , number concentration of particles/aggregates in solution ( $\text{m}^{-3}$ );  $D_i$ , fractal dimension of aggregates;  $D_{\text{FS}}$ , diffusion coefficient of fulvic molecules ( $\text{m}^2 \text{ s}^{-1}$ );  $D$ , diffusion coefficient of each particle/aggregate having radius  $r$  ( $\text{m}^2 \text{ s}^{-1}$ );  $D_{\text{min}}$ , minimum value of diffusion coefficient of particles/aggregates ( $\text{m}^2 \text{ s}^{-1}$ );  $D_{\text{max}}$ , maximum value of diffusion coefficient of particles/aggregates ( $\text{m}^2 \text{ s}^{-1}$ );  $D_X$ , diffusion coefficient of species X ( $\text{m}^2 \text{ s}^{-1}$ );  $\{\text{FeOOH}\}$ , total mass concentration of particulate  $\text{FeOOH}$  ( $\text{kg dm}^{-3}$ );  $\{\text{FS}\}$ , total concentration of fulvics ( $\text{kg C dm}^{-3}$ );  $J_t$ , total metal flux at steady-state ( $\text{mol m}^{-2} \text{ s}^{-1}$ );  $J_i$ , individual flux of the complex  $\text{Cu}^i\text{L}$  ( $\text{mol m}^{-2} \text{ s}^{-1}$ );  $J_{\text{cum}}$ , cumulative flux of particles/aggregates with radius between  $r_{\text{min}}$  and  $r$  ( $\text{mol m}^{-2} \text{ s}^{-1}$ );  $J_{\text{lab}}$ , flux obtained when all complexes are assumed to be fully labile ( $\text{mol m}^{-2} \text{ s}^{-1}$ );  $k_a$ , effective association rate constant of  $\text{Cu}^i\text{L}$  ( $\text{m}^3 \text{ mol}^{-1} \text{ s}^{-1}$ );  $k_d$ , effective dissociation rate constant of  $\text{Cu}^i\text{L}$  ( $\text{s}^{-1}$ );  $K$ , stability constant of  $\text{Cu}^i\text{L}$  ( $\text{m}^3 \text{ mol}^{-1}$ );  $K^*$ , differential equilibrium function describing the equilibrium of the metal with the whole of fulvics ( $\text{M}^{-1}$ );  $K_0^*$ , value of  $K^*$  when  $[\text{M}]_i/\{\text{FS}\} = 1 \text{ mol kg}^{-1}$  ( $\text{M}^{-1}$ );  $\{P\}_i$ , total concentration of the major component P in particles/aggregates ( $\text{kg dm}^{-3}$ );  $r$ , radius of particles/aggregates of class  $j$  (m);  $r_{\text{min}}$ , minimum radius of particles/aggregates (m);  $r_{\text{max}}$ , maximum radius of particles/aggregates (m);  $[\text{X}]^*$ , bulk concentration of species X ( $\text{mol m}^{-3}$ );  $[\text{X}]_i$ , total concentration of species X ( $\text{mol m}^{-3}$ );  $\beta$ , constant parameter of the Pareto law describing the size distribution of particles/aggregates;  $\Gamma$ , constant parameters ( $0 < \Gamma < 1$ ) describing the chemical heterogeneity of fulvics;  $\delta$ , diffusion layer thickness (m);  $\xi$ , degree of lability of  $\text{Cu}^i\text{L}$ .

## Acknowledgments

The Swiss National Foundation is gratefully acknowledged for its support (project No. 200020-101974/1). J. G. thanks the support from the Spanish Ministry of Education and Science (CTQ2006-14385).

## Supporting Information Available

Detailed tables of input and intermediate parameters for individual flux computation of Cu(II) aggregate complexes, in a Pareto size distribution, are available free of charge via the Internet at <http://pubs.acs.org>.

## Literature Cited

- (1) Alemani, D.; Buffle, J.; Zhang, Z.; Galceran, J.; Chopard, B. Metal flux and dynamic speciation at (bio)interfaces. Part III: MHE-DYN, a general code for metal flux computation; application to simple and fulvic complexants. *Environ. Sci. Technol.* **2008**, *42*, 2021–2027.
- (2) Alemani, D.; Chopard, B.; Galceran, J.; Buffle, J. LBGC method coupled to time splitting technique for solving reaction-diffusion processes in complex systems. *Phys. Chem. Chem. Phys.* **2005**, *7*, 3331–3341.
- (3) Alemani, D.; Chopard, B.; Galceran, J.; Buffle, J. Two grid refinement methods in the lattice Boltzmann framework for reaction–diffusion processes in complex systems. *Phys. Chem. Chem. Phys.* **2006**, *8*, 4119–4131.
- (4) Alemani, D. A Lattice Boltzmann numerical approach for modelling reaction-diffusion processes in chemically and physically heterogeneous environments. Ph.D. Thesis, University of Geneva, 2007.

- (5) Buffle, J.; Tercier-Waeber, M. L. Voltammetric environmental trace-metal analysis and speciation: from laboratory to in situ measurements. *TrAC, Trends Anal. Chem.* **2005**, *24*, 172–191.
- (6) van Leeuwen, H. P.; Town, R. M.; Buffle, J.; Cleven, R.; Davison, W.; Puy, J.; van Riemsdijk, W. H.; Sigg, L. Dynamic speciation analysis and Bioavailability of metals in Aquatic Systems. *Environ. Sci. Technol.* **2005**, *39*, 8545–8585.
- (7) Physicochemical Kinetics and Transport at Biointerfaces. In *IUPAC Series on Analytical and Physical Chemistry of Environmental Systems*; van Leeuwen, H. P. and Köster, W. Eds.; John Wiley & Sons: Chichester, 2004; Vol. 9.
- (8) Buffle, J.; Zhang, Z.; Startchev, K. Metal flux and dynamic speciation at (bio)interfaces. Part I: Critical evaluation and compilation of physico-chemical parameters for complexes with simple ligands and fulvic/humic substances. *Environ. Sci. Technol.* **2007**, *41*, 7609–7620.
- (9) Zhang, Z.; Buffle, J.; Alemani, D. Metal flux and dynamic speciation at (bio)interfaces. Part II: Evaluation and compilation of physicochemical parameters for complexes with particules and aggregates. *Environ. Sci. Technol.* **2007**, *41*, 7621–7631.
- (10) Galceran, J.; Puy, J.; Salvador, J.; Cecília, J.; Mas, F.; Garcés, J. L. Lability and mobility effects on mixtures of ligands under steady-state conditions. *Phys. Chem. Chem. Phys.* **2003**, *5*, 5091–5100.
- (11) Filella, M.; Buffle, J. Factors controlling the stability of submicron colloids in natural waters. *Colloids Surf. A* **1993**, *73*, 255–273.
- (12) Buffle, J.; Startchev, K.; Galceran, J. Computing steady-state metal flux at microorganism and bioanalytical sensor interfaces in multiligand systems. A reaction layer approximation and its comparison with the rigorous solution. *Phys. Chem. Chem. Phys.* **2007**, *9*, 2844–2855.
- (13) Galceran, J.; Puy, J.; Salvador, J.; Cecília, J.; van Leeuwen, H. P. Voltammetric lability of metal complexes at spherical microelectrodes with various radii. *J. Electroanal. Chem.* **2001**, *505*, 85–94.
- (14) Salvador, J.; Garcés, J. L.; Galceran, J.; Puy, J. Lability of a mixture of metal complexes under steady-state planar diffusion in a finite domain. *J. Phys. Chem. B* **2006**, *110*, 13661–13669.

ES702989V